Published in final edited form as:
Bioconjug Chem. 2011 August 17; 22(8): 1715–1722. doi:10.1021/bc2003742.

Evaluation of ^{99m}Tc-Labeled Cyclic RGD Peptide with a PEG_4 Linker for Thrombosis Imaging: Comparison with DMP444

Wei Fang[1], **Jia He**[1], **Young-Seung Kim**[2], **Yang Zhou**[2], and **Shuang Liu**[2,*]

[1]Department of Nuclear Medicine, Cardiovascular Institute & Fu Wai Hospital, Chinese Academy of Medical Science & Peking Union Medical College, Beijing, China

[2]School of Health Sciences, Purdue University, West Lafayette, USA

Abstract

DMP444 is a ^{99m}Tc-labeled cyclic RGD peptide, which has been evaluated in pre-clinical canine deep vein thrombosis (DVT) and pulmonary embolism (PE) models, and in patients with DVT and PE by SPECT (single photon emission computed tomography). Clinical data indicated that DMP444 is useful for imaging DVT; but it had limited utility for imaging PE in patients. To understand its clinical findings, we prepared a new radiotracer P4-DMP444 by replacing the lipophilic 6-aminocaproic acid (CA) in DMP444 with a highly water-soluble PEG_4 (15-amino-4,7,10,13-tetraoxapentadecanoic acid) linker. The objective of this study was to explore the impact of PEG_4 on biological properties (biodistribution, excretion kinetics and capability to image thrombi) of ^{99m}Tc radiotracer. We also used canine DVT and PE models to perform imaging studies with/without the heparin pre-treatment. These studies were specifically designed to explore the impact of heparin treatment on thrombosis uptake of P4-DMP444. It was found that replacing the CA linker with PEG_4 could enhance the radiotracer clearance kinetics from blood and normal organs in both rats and dogs. The fact that P4-DMP444 and DMP444 share very similar thrombosis uptake in both DVT and PE models suggests that the PEG_4 linker has little effect on GPIIb/IIIa binding affinity of cyclic RGD peptide. Even though P4-DMP444 had less accumulation than DMP444 in the blood, heart, lungs and muscle over the 2 h study period in both rats and dogs, their difference in PE/lung and DVT/muscle ratios is marginal, suggesting that one PEG_4 linker is not sufficient to dramatically change the contrast between thrombus and background. It is very important to note that the heparin treatment of dogs with DVT and PE resulted in dramatic decrease in accumulation of P4-DMP444 in fresh thrombi. On the basis of these results, we believe that both DMP444 and P4-DMP444 is an excellent radiotracer for imaging both DVT and PE, and should be used in patients without anti-thrombosis treatment at the time of imaging.

INTRODUCTION

Deep vein thrombosis (DVT) is the formation of blood clots in veins and is also known as venous thromboembolism.[1–3] DVT occurs when a thrombus forms in one of large veins in the lower extremities, leading to partially or completely blocked blood circulation. The condition may result in complications, such as a pulmonary embolism (PE) or death if not diagnosed and treated effectively. A majority of DVT patients will experience PE (~30% are symptomatic, and 40% are asymptomatic and at high risk) because the blood clot is unstable and can travel to and lodges in the lungs. More than one million people in the United States suffer from DVT every year. Complications from DVT kill almost 300,000 people a year –

*To whom correspondence should be addressed. Dr. Shuang Liu, School of Health Sciences, Purdue University, West Lafayette, IN 47907-2051. Phone: 765-494-0236; Fax 765-496-3367; liu100@purdue.edu.

more than AIDS and breast cancer combined.[1,3] Thus, accurate early detection of DVT and PE is highly desirable so that various therapeutic regimens can be given.

Contrast-enhanced venography remains the gold standard for diagnosis of DVT, but compression ultrasonography is the most common technique used to detect DVT in the lower extremities. The main limitation of these procedures is that neither technique can distinguish between chronic and unstable thrombi.[1,4,5] Contrast venography and ultrasonography are imaging procedures that detect changes in venous anatomy. However, these procedures may overestimate the presence of active clots.[3] Nuclear imaging by single-photon emission computed tomography (SPECT) and positron emission tomography (PET) has the potential to furnish functional information on cell biologic events which determine the risk of plaque rupture and thrombosis formation.[6–8] Radiolabeled antibodies have been used to target the fibrin and activated platelets on acute thrombi in humans,[9–15] but they have limited clinical usage due to their long blood circulation time and radioactivity accumulation in the lungs. These limitations can be alleviated by using small peptides that are cleared quickly from the blood circulation.[16–33] Examples of small peptide radiotracers include ^{99m}Tc-apcitide[16–22] and DMP444,[23–32] both of which target GPIIb/IIIa receptors on the activated platelets. ^{99m}Tc-TP850 is a ^{99m}Tc-labeled small peptide targeting the fibrin component of thrombi.[33] The ^{99m}Tc-labeled peptide radiotracers have been reviewed extensively.[34–39]

Activated platelets express GPIIb/IIIa receptors which recognize proteins and small peptides bearing RGD (arginine-glycine-glutamic acid) tripeptide sequences while non-activated platelets express no GPIIb/IIIa receptors in their active conformation.[25] DMP444 (Figure 1) is a ^{99m}Tc-labeled cyclic RGD peptide,[23] and has been evaluated extensively in pre-clinical animal models,[24–30] and in the patients with DVT and PE.[31,32] Among the ^{99m}Tc radiotracers evaluated in canine DVT models, DMP444 had the best thrombus uptake, thrombus/blood and thrombus/muscle ratios.[24] It was reported that DMP444 has higher thrombus uptake and better thrombus-to-background ratios than ^{99m}Tc-apcitide.[25] It was also found that microthromboemboli could be detected after primary percutaneous transluminal coronary angioplasty, and the infarct size was proportional to the magnitude and extent of microthromboemboli.[30] At 10 – 40 min post-injection (p.i.), eight of ten patients with suspected DVT demonstrated an area of the increased radioactivity that was clearly related to the abnormality as noted by ultrasound methods.[31] On the basis of clinical data, it was concluded that DMP444 is useful for imaging DVT; but it had very limited utility for imaging PE in patients.[31,36,37] Its lack of sensitivity and specificity might be caused either by anti-thrombosis treatment (heparin alone or combination with Coumadin®) in the patients suspected with thrombosis at the time of imaging[31] or by its slow blood clearance (45 % of the injected dose at 2 h p.i. in the canine model) and lung radioactivity accumulation.[24,25]

To understand these clinical findings, we have prepared a new radiotracer P4-DMP444 (Figure 1) by replacing the lipophilic 6-aminocaproic acid (CA) linker in DMP444 with a highly water-soluble PEG_4 (15-amino-4,7,10,13-tetraoxapentadecanoic acid). The main purpose of using PEG_4 linker was to reduce radioactivity accumulation in the blood pool and lungs while maintaining high thrombosis uptake of ^{99m}Tc radiotracer. PEG_4 has been successfully used to improve excretion kinetics of many radiolabeled small peptides.[38–44] In addition, we also used the canine DVT and PE models to perform imaging studies in the dogs with/without heparin pre-treatment. These studies were specifically designed to explore the impact of heparin treatment on thrombosis uptake of P4-DMP444. In this report, we present biological evaluations of P4-DMP444 in the rat and dog models.

EXPERIMENTAL

Materials and Instruments

Chemicals were purchased from *Sigma/Aldrich* (St. Louis, MO), and were used without further purification. Cyclic RGD peptide c[R(Me)GDV(Mamb(PEG_4))] (P4-DMP757) was custom-made by Peptides International, Inc. (Louisville, KY). Succinimidyl 6-(2-(2-sulfonatobenzaldehyde)hydrazono)nicotinate (HYNIC-NHS), HYNIC-c[R(Me)GDV(Mamb(CA)] (HYNIC-CA-DMP757) and [^{99m}Tc(HYNIC-CA-DMP757)(tricine)(TPPTS)] (DMP444) were prepared according to the procedures described in our previous report.[23] $Na^{99m}TcO4$ was obtained from a commercial Lantheus $^{99}Mo/^{99m}Tc$ Technelite® generator (North Billerica, MA). The ESI (electrospray ionization) mass spectral data were collected on a Finnigan LCQ classic mass spectrometer, School of Pharmacy, Purdue University.

HPLC Methods

The semi-prep HPLC method (Method 1) used a LabAlliance HPLC system equipped with a UV/vis detector (λ = 254 nm) and Zorbax C_{18} semi-prep column (9.4 nm x 250 mm, 100 Å pore size; Agilent Technologies, Santa Clara, CA). The flow rate was 2.5 mL/min and the mobile phase was isocratic with 70% A (0.1% TFA in water) and 30% B (0.1% TFA in methanol) at 0 – 5 min, followed by a gradient mobile phase going from 30% B at 5 min to 70% B at 20 min. The radio-HPLC method (Method 2) used the LabAlliance HPLC system equipped with a β-ram IN/US detector (Tampa, FL) and Zorbax C_{18} column (4.6 mm x 250 mm, 300 Å pore size; Agilent Technologies, Santa Clara, CA). The flow rate was 1 mL/min with a gradient mobile phase started with 90% A (25 mM NH_4OAc, pH = 6.8) and 10% B (acetonitrile) to 85% A and 15% B at 5 min, followed by another gradient mobile phase going from 15% B at 5 min to 20% B at 20 min and to 60% B at 25 min.

HYNIC-P4-DMP757

HYNIC-NHS (5.8 mg, 13 μmol) and PEG_4-DMP757 (2.2 mg, 2.6 μmol) were dissolved in anhydrous DMF (2 mL). To the mixture above was added diisopropylethylamine (DIEA: 3 drops). The reaction mixture was then stirred at room temperature for 20 h. After addition of 2 mL water and 2 drops of acetic acid, the solution was subjected to HPLC purification (Method 1). Fractions at 14.26 min were collected. Lyophilization of the combined collections afforded the expected product HYNIC-P4-DMP757 as a white powder 1.7 mg (yield 57.4%). ESI-MS: m/z = 1162 for $[M + Na]^+$ (1139.5 calcd. for $[C_{50}H_{69}N_{13}O_{16}S]$).

^{99m}Tc-Labeling and Dose Preparation

To a clean 5 cc vial filled with 1.0 mL solution (pH = 4.8) containing 5 mg TPPTS, 6.5 mg tricine, 40 mg mannitol, 38.5 mg disodium succinate hexahydrate, and 12.7 mg succinic acid, were added 0.2 mL of the HYNIC-peptide conjugate solution (100 μg/mL in water) and 0.3 mL of $Na^{99m}TcO_4$ (10 – 30 mCi/mL) in saline. The vial was heated at 100 °C for 20 min in a lead-shielded water bath. After radiolabeling, the vial was placed back into the lead pig, and allowed to stand at room temperature for 5 – 10 min. A sample of the resulting solution was analyzed by radio-HPLC (Method 2). The Log P values were determined using the literature procedure.[46, 47] For biodistribution studies, all new radiotracers were prepared and purified by radio-HPLC. Volatiles in the HPLC mobile phase were removed under vacuum. Doses were prepared by dissolving the HPLC-purified radiotracer in saline to a concentration of ~30 μCi/mL. For imaging studies, doses were prepared by dissolving the radiotracer in saline to 1 – 5 mCi/mL depending upon the animals (rats versus dogs). The resulting solution was filtered with a 0.20 micron Millex-LG filter to remove any foreign particles before being injected into animals.

Biodistribution Protocol

Biodistribution studies were performed using Sprague-Dawley (SD) rats in compliance with the NIH animal experiment guidelines (*Principles of Laboratory Animal Care*, NIH Publication No. 86-23, revised 1985). The animal protocol was approved by the Purdue University Animal Care and Use Committee. In short, 16 SD rats (200 – 250 g) were anesthetized with intramuscular injection of a mixture of ketamine (80 mg/kg) and xylazine (19 mg/kg). Each animal was administered with ~3 μCi of ^{99m}Tc radiotracer by tail vein injection. Four animals were sacrificed by sodium pentobarbital overdose (~200 mg/kg) at 5, 30, 60, and 120 min post-injection (p.i.). Blood samples were withdrawn from the heart of rats. The brain, eyes, heart, spleen, lungs, liver, kidneys, muscle and intestine were harvested, washed with saline, dried with absorbent tissue, weighed, and counted on a Perkin Elmer Wizard – 1480 γ-counter (Shelton, CT). The organ uptake was calculated as the percentage of injected dose per gram of organ mass (%ID/g). Biodistribution data (%ID/g) are reported as an average plus the standard variation based on the results from four animals. Comparison between two radiotracers was made using the two-way ANOVA test (GraphPad Prim 5.0, San Diego, CA). The level of significance was set at $p < 0.05$.

Animal Preparation for Studies in Dogs

All experiments were performed in accordance with the NIH animal experiment guidelines (*Principles of Laboratory Animal Care*, NIH Publication No. 86-23, revised 1985). The protocols for animal studies in dogs have been approved by the Fu Wai Hospital Animal Care and Use Committee (Beijing, China). Five adult mongrel dogs (20.6 ± 1.8 kg, range 18~25 kg, fasted overnight) were anesthetized with intravenous (i.v.) injection of a mixture of ketamine (25 mg/kg) and diazepam (1.1 mg/kg), incubated with a cuffed endotracheal tube, and ventilated on a respirator with positive end-expiratory pressure of 4 cm H_2O. Additional sodium pentobarbital were used via i.v. injection to maintain anesthesia, when needed.

Blood Clearance Kinetics in Normal Dogs

Once under anesthesia, each animal was administered with 370 MBq of ^{99m}Tc radiotracer via the femoral vein. Venous blood samples (2 mL) were collected via a femoral vein catheter at 0.5, 2, 3, 4, 5, 10, 15, 30, 60, 90 and 120 min post-injection. The collected blood samples were weighed and counted for radioactivity in a gamma-counter (FT-646, Beijing Nuclear Instrument Factory, China). The radioactivity counts were corrected for radiation decay.

Planar Imaging in Normal Dogs

Once the animal was under anesthesia, it was placed supine on a dual-head γ-camera (E-cam, Siemens Medical Systems, Hoffman Estates, IL) equipped with a parallel-hole, low-energy, high-resolution collimator and 20% window centered on the 140 keV ^{99m}Tc photopeak. After administration of P4-DMP444 (~370 MBq) via the contralateral femoral vein, anterior planar images were acquired at 5, 15, 30, 60, 90 and 120 min p.i., and were stored digitally in a 128×128 matrix. The acquisition count limits were set at 500 K. After completion of imaging, animals were allowed to recover at the Center for Experimental Animals (Fu Wai Hospital). To quantify images, regions of interest (ROIs) were drawn around heart, lung and liver on each image acquired at each time-point. The raw radioactivity data in each ROI was expressed as counts/pixel per min. For comparison purposes, DMP444 was also evaluated for blood clearance and planar imaging in normal dogs using the same injection dose and same protocol. The time interval between two imaging studies for P4-DMP444 and DMP444 in the same dogs was at least 24 hours.

Deep Venous Thrombosis (DVT) Model

^{99m}Tc radiotracers were evaluated in vivo in canine model which has been reported previously for the evaluation of thrombus imaging radiotracers.[17,45] Five adult mongrel dogs were anesthetized with intravenous injection of a mixture of ketamine (25 mg/kg) and diazepam (1.1 mg/kg). In each animal, an 18-gauge angiocath was inserted into the distal half of right femoral vein and a 10-mm two-stranded spiral stainless steel coil was placed in the femoral vein at approximately the mid-femur. The catheter was then removed, the wound was sutured and the placement of the coils was documented by radiograph.

Pulmonary Embolism (PE) Model

Five adult mongrel dogs were anesthetized with pentobarbital (30mg/kg) administered by intravenous injection. A 10-mm two-stranded spiral stainless steel embolization coil was inserted into left lower pulmonary artery through catheter in each dog. At 30min after coil placement, X-ray angiography was performed to document the pulmonary embolism and the locations of the coils. After catheter was removed, the wound was sutured. During the operation for generating pulmonary embolism, the dogs were anesthetized, and electrocardiogram (ECG) and SaO_2 were recorded. ECG was changed during the insertion of catheter and was recovered quickly after removal. All animals were allowed to recover for 24 h before imaging with ^{99m}Tc radiotracer. There was no animal death before the completion of imaging.

Thrombus imaging

The animal was placed supine under a SPECT camera (SIEMENS, Germany) which was equipped with a low-energy, all-purpose collimator and set to acquire the 140 keV photopeak of ^{99m}Tc with a 20% window. ^{99m}Tc radiotracer (~370 MBq) were injected intravenously into a foreleg line and flushed in with saline. The 30° left anterior oblique images over the chest region (for PE) or the anterior images over leg (for DVT) were acquired at 15, 30, 60, 90 and 120 min p.i. The total counts over the chest region (for PE model) or the leg (for DVT model) were set up to 500,000. From the computer-stored images, thrombus-to-background ratios were determined. Average counts per pixel were computed from ROIs drawn manually around the areas of known thrombus (corresponding to the locations of coils in radiographs). ROIs were drawn over the thrombus-containing lung to evaluate adjacent lung background for PE models. The PE/Lung ratios were determined by dividing mean counts per pixel for PE by mean counts per pixel for lung background. Similarly, ROIs were drawn over both medial and lateral thigh in the thrombus-containing leg to calculate the muscle background for DVT models. The DVT/muscle ratios were determined by dividing mean counts per pixel for DVT by mean counts per pixel for muscle (average of medial and lateral ROIs).

Heparin Treatment on Radiotracer Thrombus Uptake

Two mongrel dogs with the PE were used to explore the impact of heparin treatment on the pulmonary thrombus uptake of P4-DMP444. A dose of 200 units/kg heparin (Changzhou Qianhong Bio-Pharma Co. Ltd., China) was intravenously injected at 10 min before the embolization coil was placed into left lower pulmonary artery. The chest region imaging protocol was performed as aforementioned.

Statistical Analysis

Statistical computations and analysis were made with SPSS 13.0 software (SPSS Inc, Chicago, IL). The results are expressed as mean ± SD. Changes between the means within a group at different time points were assessed with one-way repeated-measures ANOVA test.

Comparison between two radiotracers was made with 2-way ANOVA test. The level of significance was set at $p < 0.05$.

RESULTS

HYNIC Conjugate Synthesis

Synthesis of HYNIC-P4-DMP757 was straightforward by reacting P4-DMP757 with excess HYNIC-OSu in anhydrous DMF in the presence of base, such as DIEA. It was purified from the reaction mixture by semi-prep HPLC. Its composition has been confirmed by ESI-MS, and is completely consistent with the proposed structure (Figure 1). Its HPLC purity was > 95% before being used for ^{99m}Tc-labeling.

Radiochemistry

P4-DMP444 was prepared according to the same method for DMP444.[23] No significant ^{99m}Tc-colloid (<0.5%) was detected using the non-$SnCl_2$ formulation, in which TPPTS acts as a reducing agent for $^{99m}TcO_4^-$ and a coligand at the same time to stabilize the ^{99m}Tc-HYNIC core. The partition coefficients of P4-DMP444 and DMP444 were determined in an equal volume mixture of 1-octanol and 25 mM phosphate buffer (pH = 7.4). The calculated log P values for P4-DMP444 and DMP444 were −3.96 ± 0.20 and −4.02 ± 0.16, respectively. Apparently, there was no significant difference in their lipophilicity.

Biodistribution Properties

SD rats were used to compare biodistribution patterns of DMP444 and P4-DMP444. This animal model was used to evaluate peptide radiotracers, such as ^{99m}Tc-apcitide.[16,17] The selected biodistribution data are listed in Tables SI1 and SI2, respectively. Figure 2 compares organ uptake of P4-DMP444 and DMP444 in blood, heart, lungs and muscle of SD rats. We are particularly interested in these organs because the radioactivity accumulation in the blood and heart will have significant impact on detection of arterial thrombi, in the lungs for PE, and in the muscle for DVT. The uptake of P4-DMP444 and DMP444 was low in the blood, heart, lung and muscle. At 5 min p.i., P4-DMP444 had significantly lower ($p < 0.05$) uptake than DMP444. However, this difference disappeared at later times (>15 min p.i.). It was clear that replacing the CA linker with PEG_4 resulted in lower radioactivity accumulation in normal organs. These promising data led us to explore the blood clearance kinetics and biodistribution patterns of P4-DMP444 and DMP444 in dogs.

Blood Clearance Kinetics

Figure 3 shows blood clearance curves of P4-DMP444 and DMP444 in normal dogs. The radioactivity is expressed as a percentage of initial radioactivity level at 30 seconds p.i. Clearly, P4-DMP444 had faster blood clearance with >50% of initial radioactivity remaining at 5 min p.i. and 24.6% of initial radioactivity remaining at 120 min p.i. In contrast, DMP444 had nearly 50% of initial radioactivity remaining at 10 min p.i. and 34.6% of initial radioactivity remaining at 120min p.i. ($p < 0.05$ for P4-DMP444 vs. DMP444 at 120 min p.i.)

Planar Imaging in Normal Dogs

Figure 4 illustrates the clearance kinetics of P4-DMP444 and DMP444 from normal organs in dogs. The radioactivity in the heart, lung and liver decreased markedly for both P4-DMP444 and DMP444 over the 2 h study period. P4-DMP444 had faster clearance than that

of DMP444 from the heart, lung and liver. There was a significant uptake difference ($p < 0.05$) between P4-DMP444 and DMP444 in the heart, lung and liver at 120 min p.i.

Thrombus Imaging in Canine DVT and PE Models

Figure 5 compares the DVT (top: in right femoral vein) and PE (bottom: in the left lung) images obtained in dogs administered with P4-DMP444 and DMP444. Figure 6 shows the comparison of their PE/lung and DVT/muscle ratios at 15, 30, 60, 90 and 120 min p.i. in canine PE and DVT models. The lower uptake in the heart and lungs were observed for P4-DMP444. The PE/lung and DVT/muscle ratios were improved steadily from 15min to 120min p.i. P4-DMP444 had a significantly higher PE/lung ratio than DMP444 at 120min p.i. (4.04 ± 0.13 vs 3.72 ± 0.14, $p < 0.05$). The difference between P4-DMP444 and DMP444 was not statistically significant for their DVT/muscle ratios (4.56 ± 0.41 vs 4.38 ± 0.28, $p > 0.05$) at 120min p.i.

Impact of Heparin on Thrombus Uptake

Figure 7 shows planar images of the chest region in the dogs with PE (top: in the right lung) and DVT (bottom: in the right thigh) at 120 min after injection of P4-DMP444 with (right) and without (left) the anti-thrombosis treatment. It was quite clear that pre-treatment of the dog with heparin at a dose of 200 units/kg significantly reduced the DVT and PE uptake of P4-DMP444.

DISCUSSION

In this study, we compared the biodistribution properties of DMP444 and P4-DMP444 (Figure 1) and their excretion kinetics from normal organs of the rats (Figure 2) and dogs (Figure 3). We are surprised to find out that replacing the lipophilic CA linker with PEG_4 had little effect on lipophilicity of ^{99m}Tc radiotracers (log $P = -3.96 \pm 0.20$ for P4-DMP444 and -4.02 ± 0.16 for DMP444). However, using the PEG_4 linker resulted in lower radioactivity accumulation in normal organs (e.g. blood, heart, liver and lungs) of rats and dogs. These results are consistent with those obtained with radiolabeled PEG_4–containing small peptides in our previous studies.[38–44]

We also compared their capability to image thrombi in canine DVT and PE models. The fact that P4-DMP444 and DMP444 share similar thrombosis uptake (Figure 5) strongly suggests that replacing the CA linker with PEG_4 has little impact on GPIIb/IIIa binding affinity of cyclic RGD peptide. On the basis of their clearance kinetics from the blood, heart, liver and lungs (Figures 3 and 4), one might expect better DVT/muscle and PE/lung ratios for P4-DMP444 as compared to DMP444. However, we found that P4-DMP444 and DMP444 shared very similar DVT/muscle ratios (Figure 6), probably because they both had low muscle uptake (Tables SI1 and SI2). Even though P4-DMP444 seems to have better PE/lung ratios (Figure 6) than DMP444 over the 2 h study period, their difference is marginal, suggesting that the addition of only one PEG_4 linker is not sufficient to dramatically change the contrast between thrombus and background, particularly muscle and lungs. Due to their very low lung uptake (Tables SI1 and SI2), it is reasonable to believe that the radioactivity accumulation in lungs is not the key factor contributing to the limited utility of DMP444 for imaging PE in patients.

Heparin is a naturally-occurring anticoagulant that prevents the formation of blood clots and extension of existing clots within the blood. Heparin and its low molecular weight derivatives (e.g. enoxaparin, dalteparin, tinzaparin) are used as anti-thrombosis agents to prevent DVT and PE in patients at risk.[48] In fact, most of the patients suspected with thrombosis take heparin alone or in combination with Warfarin® (Coumadin®) at the time

of imaging.[31,36] Thus, we explored the impact of heparin treatment on imaging quality in the dogs administered with P4-DMP444. In this study, we found that the heparin treatment in dogs with DVT and PE before administration of P4-DMP444 resulted in dramatic decrease in radioactivity accumulation in the fresh thrombi (Figure 7). While heparin does not break down clots that have already formed, it allows the body's natural clot lysis mechanisms to work normally to break down blood clots that have formed. It is well-established that heparin binds to the enzyme inhibitor antithrombin III (AT) causing a conformational change, resulting in its activation through an increase in the flexibility of its reactive site loop.[49,50] The activated AT then inactivates thrombin and other proteases involved in blood clotting, most notably factor Xa,[49,50] which often leads to the deactivation of platelets and related receptors, such as GPIIb/IIIa. The rate of inactivation of these proteases by AT can increase by up to 1000-fold due to the binding of heparin.[57] Thus, it is not surprising that DMP444 has very limited utility for imaging PE in the patients who were on anti-thrombosis medication at the time of imaging.[35,36] We believe that DMP444 and P4-DMP444 will have better sensitivity and specificity in the DVT and PE patients without anti-thrombosis treatment (heparin alone or in combination with Warfarin®).

CONCLUSION

In this study, we found that replacing the CA linker with PEG_4 can improve the excretion kinetics from normal organs (blood, heart, liver and lungs). Even though P4-DMP444 seems to have better PE/lung ratios than DMP444 over the 2 h study period, the addition of one PEG_4 linker in P4-DMP444 is not sufficient to dramatically change the contrast between thrombus and background. It is very important to note that the heparin pre-treatment of dogs with DVT and PE can result in dramatic decrease in radioactivity accumulation in fresh thrombi. On the basis of the results from this study, we believe that P4-DMP444 is an excellent radiotracer for imaging both DVT and PE, and should be used in the patients without anti-thrombosis treatment at the time of imaging.

Acknowledgments

This work is supported, in part, by Purdue University and the research grant R01 CA115883 from the National Cancer Institute (NCI).

LITERATURE CITED

1. Blum JE, Handmaker H. Small peptide radiopharmaceuticals in the imaging of acute thrombus. Curr Pharm Des. 2002; 8:1815–1826. [PubMed: 12171533]
2. Quinn MJ, Byzova TV, Qin J, Topol EJ, Plow EF. Integrin $\alpha_{IIb}\beta_3$ and its antagonism. Arterioscler Thromb Vasc Biol. 2003; 23:945–952. [PubMed: 12637342]
3. Chan WS, Ginsberg JS. Diagnosis of deep vein thrombosis and pulmonary embolism in pregnancy. Thromb Res. 2002; 107:85–91. [PubMed: 12431472]
4. Nissen SE, Yock P. Intravascular ultrasound: novel pathophysiological insights and current clinical applications. Circulation. 2001; 103:604–616. [PubMed: 11157729]
5. Caussin C, Ohanessian A, Ghostine S, Jacq L, Lancelin B, Dambrin G, Sigal-Cinqualbre A, Angel CY, Paul JF. Characterization of vulnerable nonstenotic plaque with 16-slice computed tomography compared with intravascular ultrasound. Am J Cardiol. 2004; 94:99–104. [PubMed: 15219516]
6. de Feyter PJ, Nieman K. New coronary imaging techniques: what to expect? Heart. 2002; 87:195–197. [PubMed: 11847148]
7. Jaffer FA, Libby P, Weissleder R. Molecular and cellular imaging of atherosclerosis: emerging applications. J Am Coll Cardiol. 2006; 47:1328–1338. [PubMed: 16580517]
8. Choudhury RP, Fuster V, Fayad ZA. Molecular, cellular and functional imaging of atherothrombosis. Nat Rev Drug Discov. 2004; 3:913–925. [PubMed: 15520814]

9. Moriwaki H, Matsumoto M, Handa N, Isaka Y, Hashikawa K, Oku N, Nakamura M, Kamada T, Nishimura T. Functional and anatomic evaluation of carotid atherothrombosis. A combined study of indium 111 platelet scintigraphy and B-mode ultrasonography. Arterioscler Thromb Vasc Biol. 1995; 15:2234–2240. [PubMed: 7489248]
10. Tsimikas S, Palinski W, Halpern SE, Yeung DW, Curtiss LK, Witztum JL. Radiolabeled MDA2, an oxidation-specific, monoclonal antibody, identifies native atherosclerotic lesions in vivo. J Nucl Cardiol. 1999; 6:41–53. [PubMed: 10070840]
11. Cerqueira MD, Stratton JR, Vracko R, Schaible TF, Ritchie JL. Noninvasive arterial thrombus imaging with ^{99m}Tc monoclonal antifibrin antibody. Circulation. 1992; 85:298–304. [PubMed: 1728460]
12. Matter CM, Schuler PK, Alessi P, Meier P, Ricci R, Zhang D, Halin C, Castellani P, Zardi L, Hofer CK, Montani M, Neri D, Lüscher TF. Molecular imaging of atherosclerotic plaques using a human antibody against the extradomain B of fibronectin. Circ Res. 2004; 95:1225–1233. [PubMed: 15539632]
13. Tsimikas S, Shortal BP, Witztum JL, Palinski W. In vivo uptake of radiolabeled MDA2, an oxidation-specific monoclonal antibody, provides an accurate measure of atherosclerotic lesions rich in oxidized LDL and is highly sensitive to their regression. Arterioscler Thromb Vasc Biol. 2000; 20:689–697. [PubMed: 10712392]
14. Shaw PX, Hörkkö S, Tsimikas S, Chang MK, Palinski W, Silverman GJ, Chen PP, Witztum JL. Human-derived anti-oxidized LDL autoantibody blocks uptake of oxidized LDL by macrophages and localizes to atherosclerotic lesions in vivo. Arterioscler Thromb Vasc Biol. 2001; 21:1333–1339. [PubMed: 11498462]
15. Ginsberg HN, Goldsmith SJ, Vallabhajosula S. Noninvasive imaging of ^{99m}technetium-labeled low density lipoprotein uptake by tendon xanthomas in hypercholesterolemic patients. Arteriosclerosis. 1990; 10:256–262. [PubMed: 2317159]
16. Muto P, Lastoria S, Varrella P, Vergara E, Salvatore M, Morgano G, Lister-James J, Bernardy JD, Dean RT, Wencker D. Detecting deep venous thrombosis with technetium-99m-labeled synthetic peptide P280. J Nucl Med. 1995; 36:1384–1391. [PubMed: 7629582]
17. Lister-James J, Knight LC, Maurer AH, Bush LR, Moyer BR, Dean RT. Thrombus imaging with a technetium-99m-labeled activated platelet receptor-binding peptide. J Nucl Med. 1996; 37:775–781. [PubMed: 8965144]
18. Bates SM, Lister-James J, Julian JA, Taillefer R, Moyer BR, Ginsberg JS. Imaging characteristics of a novel technetium Tc-99m-labeled platelet glycoprotein IIb/IIIa receptor antagonist in patients with acute deep vein thrombosis or a history of deep vein thrombosis. Arch Intern Med. 2003; 163:452–456. [PubMed: 12588204]
19. Taillefer R, Therasse E, Turpin S, Lambert R, Robillard P, Soulez G. Comparison of early and delayed scintigraphy with ^{99m}Tc-apcitide and correlation with contrast-enhanced venography in detection of acute deep vein thrombosis. J Nucl Med. 1999; 40:2029–2035. [PubMed: 10616882]
20. Carretta RF, Streek PV, Weiland FL. Optimizing images of acute deep-vein thrombosis using technetium-99m-apcitide. J Nucl Med Technol. 1999; 27:271–275. [PubMed: 10646544]
21. Taillefer R, Edell S, Innes G, Lister-James J. Acute thromboscintigraphy with ^{99m}Tc-apcitide: results of the phase 3 multicenter clinical trial comparing ^{99m}Tc-apcitide scintigraphy with contrast venography for imaging acute DVT. Multicenter trial investigators. J Nucl Med. 2000; 41:1214–1223. [PubMed: 10914912]
22. Dunzinger A, Hafner F, Schaffler G, Piswanger-Soelkner JC, Brodmann M, Lipp RW. ^{99m}Tc-apcitide scintigraphy in patients with clinically suspected deep venous thrombosis and pulmonary embolism. Eur J Nucl Med Mol Imaging. 2008; 35:2082–2087. [PubMed: 18618107]
23. Edwards DS, Liu S, Barrett JA, Harris AR, Looby RJ, Ziegler MC, Heminway SJ, Carroll TR. New and versatile ternary ligand system for technetium radiopharmaceuticals: water soluble phosphines and tricine as coligands in labeling a hydrazinonicotinamide-modified cyclic glycoprotein IIb/IIIa receptor antagonist with ^{99m}Tc. Bioconj Chem. 1997; 8:146–154.
24. Barrett JA, Crocker AC, Damphousse DJ, Heminway SJ, Liu S, Edwards DS, Lazewatsky JL, Kagan M, Mazaika TJ, Carroll TR. Biological evaluation of thrombus imaging agents utilizing water soluble phosphines and tricine as coligands to label a hydrazinonicotinamide-modified cyclic glycoprotein IIb/IIIa receptor antagonist with ^{99m}Tc. Bioconj Chem. 1997; 8:155–160.

25. Mousa SA, Bozarth JM, Edwards S, Carroll T, Barrett JA. Novel technetium-99m-labeled platelet GPIIb/IIIa receptor antagonists as potential imaging agents for venous and arterial thrombi. Coron Artery Dis. 1998; 9:131–141. [PubMed: 9647415]
26. Oyen WJ, Boerman OC, Brouwers FM, Barrett JA, Verheugt FW, Ruiter DJ, Corstens FH, van der Meer JW. Scintigraphic detection of acute experimental endocarditis with the technetium-99m labelled glycoprotein IIb/IIIa receptor antagonist DMP444. Eur J Nucl Med. 2000; 27:392–399. [PubMed: 10805111]
27. Mitchel J, Waters D, Lai T, White M, Alberghini T, Salloum A, Knibbs D, Li D, Heller GV. Identification of coronary thrombus with a IIb/IIIa platelet inhibitor radiopharmaceutical, technetium-99m DMP-444: a canine model. Circulation. 2000; 101:1643–1646. [PubMed: 10758044]
28. Scharn DM, Oyen WJ, Klemm PL, Wijnen MH, vanderVliet JA. Assessment of prosthetic vascular graft thrombogenicity using the technetium-99m labeled glycoprotein IIb/IIIa receptor antagonist DMP444 in a dog model. Cardiovasc Surg. 2002; 10:566–569. [PubMed: 12453688]
29. Sakuma T, Sari I, Goodman CN, Lindner JR, Klibanov AL, Kaul S. Simultaneous integrin $\alpha_v\beta_3$ and glycoprotein IIb/IIIa inhibition causes reduction in infarct size in a model of acute coronary thrombosis and primary angioplasty. Cardiovasc Res. 2005; 66:552–561. [PubMed: 15914120]
30. Sakuma T, Sklenar J, Leong-Poi H, Goodman NC, Glover DK, Kaul S. Molecular imaging identifies regions with microthromboemboli during primary angioplasty in acute coronary thrombosis. J Nucl Med. 2004; 45:1194–1200. [PubMed: 15235066]
31. Klem JA, Schaffer JV, Crane PD, Barrett JA, Henry GA, Canestri L, Ezekowitz MD. Detection of deep venous thrombosis by DMP 444, a platelet IIb/IIIa antagonist: a preliminary report. J Nucl Cardiol. 2000; 7:359–364. [PubMed: 10958278]
32. Brouwers FM, Oyen WJ, Boerman OC, Barrett JA, Verheugt FW, Corstens FH, Van der Meer JW. Evaluation of Tc-99m-labeled glycoprotein IIb/IIIa receptor antagonist DMP444 SPECT in patients with infective endocarditis. Clin Nucl Med. 2003; 28:480–484. [PubMed: 12911097]
33. Aruva MR, Daviau J, Sharma SS, Thakur ML. Imaging thromboembolism with fibrin-avid ^{99m}Tc-peptide: evaluation in swine. J Nucl Med. 2006; 47:155–162. [PubMed: 16391200]
34. Cerqueira MD. Current status of radionuclide tracer imaging of thrombi and atheroma. Semin Nucl Med. 1999; 29:339–351. [PubMed: 10534236]
35. Taillefer R. Radiolabeled peptides in the detection of deep venous thrombosis. Semin Nucl Med. 2001; 31:102–123. [PubMed: 11330782]
36. Bernarducci MP. Radiolabeled peptides: overcoming the challenges of post-surgical patient management of venous thromboembolism. Surg Technol Int. 2004; 12:50–67. [PubMed: 15455310]
37. Dobrucki LW, Sinusas AJ. PET and SPECT in cardiovascular molecular imaging. Nat Rev Cardiol. 2010; 7:38–47. [PubMed: 19935740]
38. Wang L, Shi J, Kim YS, Zhai S, Jia B, Zhao H, Liu Z, Wang F, Chen X, Liu S. Improving tumor-targeting capability and pharmacokinetics of ^{99m}Tc-labeled cyclic RGD dimers with PEG_4 linkers. Mol Pharm. 2009; 6:231–245. [PubMed: 19067525]
39. Shi J, Kim YS, Zhai S, Liu Z, Chen X, Liu S. Improving tumor uptake and pharmacokinetics of ^{64}Cu-labeled cyclic RGD dimers with triglycine and PEG_4 Linkers. Bioconj Chem. 2009; 20:750–759.
40. Liu S, He Z, Hsieh WY, Kim YS, Jiang Y. Impact of PKM linkers on biodistribution characteristics of the ^{99m}Tc-labeled cyclic RGDfK dimer. Bioconj Chem. 2006; 17:1499–1507.
41. Jia B, Liu Z, Shi J, Yu Z, Yang Z, Zhao H, He Z, Liu S, Wang F. Linker effects on biological properties of ^{111}In-labeled DTPA conjugates of a cyclic RGDfK dimer. Bioconj Chem. 2008; 19:201–210.
42. Liu Z, Niu G, Shi J, Liu S, Wang F, Liu S, Chen X. ^{68}Ga-labeled cyclic RGD dimers with Gly_3 and PEG_4 linkers: promising agents for tumor integrin $\alpha_v\beta_3$ PET imaging. Eur J Nucl Med Mol Imaging. 2009; 36:947–957. [PubMed: 19159928]
43. Liu Z, Liu S, Wang F, Liu S, Chen X. Noninvasive imaging of tumor integrin expression using ^{18}F-labeled RGD dimer peptide with PEG_4 linkers. Eur J Nucl Med Mol Imaging. 2009; 36:1296–1307. [PubMed: 19296102]

44. Liu S. Radiolabeled cyclic RGD peptides as integrin $\alpha_v\beta_3$-targeted radiotracers: maximizing binding affinity via bivalency. Bioconj Chem. 2009; 20:2199–2213.
45. Meoli DF, Sadeghi MM, Krassilnikova S, Bourke BN, Giordano FJ, Dione DP, Su H, Edwards DS, Liu S, Harris TD, Madri JA, Zaret BL, Sinusas AJ. Noninvasive imaging of myocardial angiogenesis following experimental myocardial infarction. J Clin Invest. 2004; 113:1684–1691. [PubMed: 15199403]
46. Agnelli G, Piovella F, Buoncristiani P, Severi P, Pini M, D'Angelo A, Beltrametti C, Damiani M, Andrioli GC, Pugliese R, Iorio A, Brambilla G. Enoxaparin plus compression stockings compared with compression stockings alone in the prevention of venous thromboembolism after elective neurosurgery. N Engl J Med. 1998; 339:80–5. [PubMed: 9654538]
47. Bergqvist D, Agnelli G, Cohen AT, Eldor A, Nilsson PE, Le Moigne-Amrani A, Dietrich-Neto F. Duration of prophylaxis against venous thromboembolism with enoxaparin after surgery for cancer. N Engl J Med. 2002; 346:975–980. [PubMed: 11919306]
48. Handoll HH, Farrar MJ, McBirnie J, Tytherleigh-Strong G, Milne AA, Gillespie WJ. Heparin, low molecular weight heparin and physical methods for preventing deep vein thrombosis and pulmonary embolism following surgery for hip fractures. Cochrane Database Syst Rev. 2002; 4:CD000305. [PubMed: 12519540]
49. Chuang YJ, Swanson R, Raja SM, Olson ST. Heparin enhances the specificity of antithrombin for thrombin and factor Xa independent of the reactive center loop sequence. Evidence for an exosite determinant of factor Xa specificity in heparin-activated antithrombin. J Biol Chem. 2001; 276:14961–14971. [PubMed: 11278930]
50. Björk I, Lindahl U. Mechanism of the anticoagulant action of heparin. Mol Cell Biochem. 1982; 48:161–182. [PubMed: 6757715]

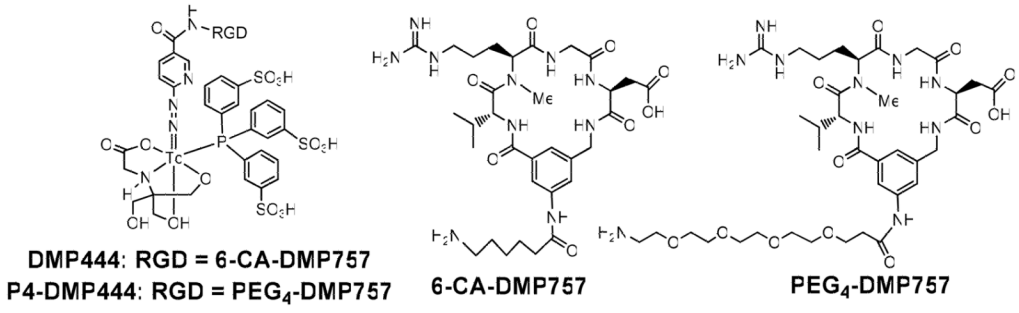

Figure 1.

Structure of cyclic RGD peptides targeting GPIIb/IIIa receptors on activated platelets, and their corresponding ternary ligand ^{99m}Tc complexes [^{99m}Tc(HYNIC-RGD)(tricine)(TPPTS)] (DMP444: RGD = 6-CA-DMP757, and CA = 6-aminocaproic acid; P4-DMP444: RGD = PEG_4-DMP757, and PEG_4 = 15-amino-4,7,10,13-tetraoxapentadecanoic acid).

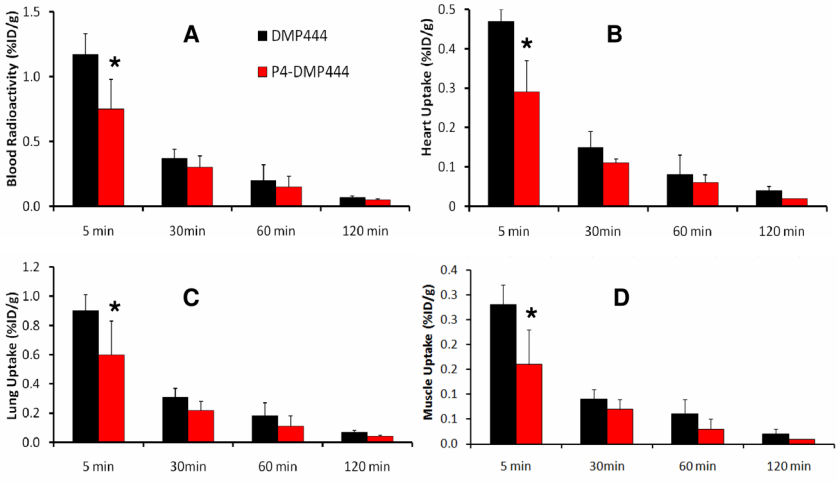

Figure 2.

Comparison of organ uptake (%ID/g) of DMP444 and P4-DMP444 in the blood (**A**), heart (**B**), Lung (**C**) and muscle (**D**) of Sprague-Dawley rats (n = 4) at 5, 30, 60 and 120 min p.i. At 5 min p.i., P4-DMP444 had significantly lower ($p < 0.05$) uptake than DMP444; but this difference disappeared at later times (>15 min p.i.).

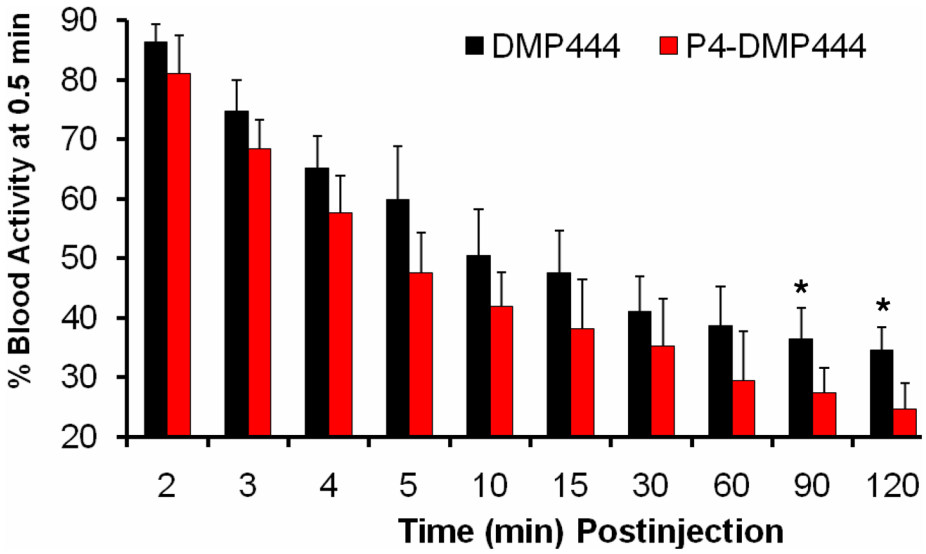

Figure 3.

Comparison of blood clearance kinetics as determined by γ-counting between DMP444 and P4-DMP444 over 2 h study period. The blood radioactivity for P4-DMP444 was significantly lower ($P < 0.05$) than that for DMP444 at >90 min p.i.

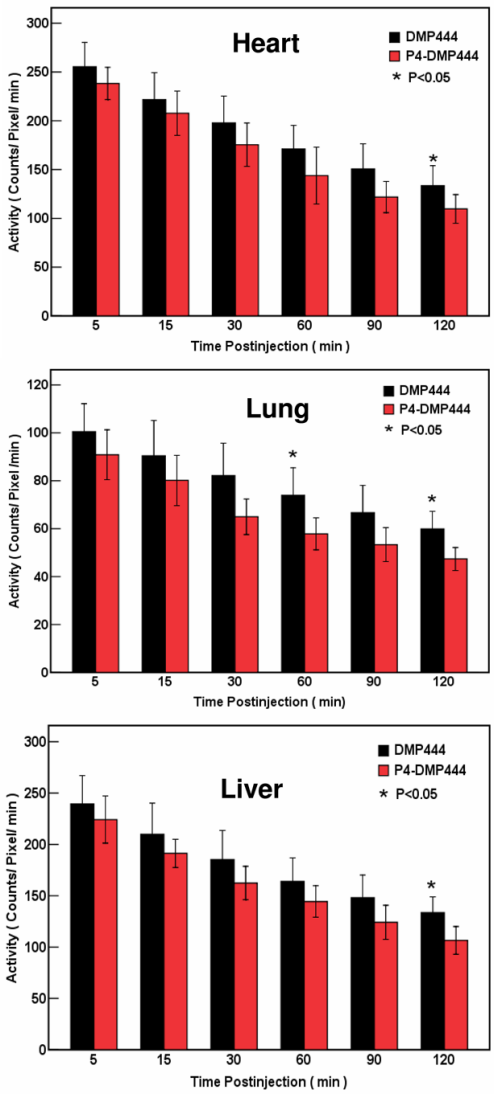

Figure 4.

Organ distribution kinetics from imaging quantification in dogs administered with DMP444 and P4-DMP444 in the heart, lungs and liver. There was significant difference ($p<0.05$) between DMP444 and P4-DMP444 for their heart, lung and liver radioactivity at 120min p.i.

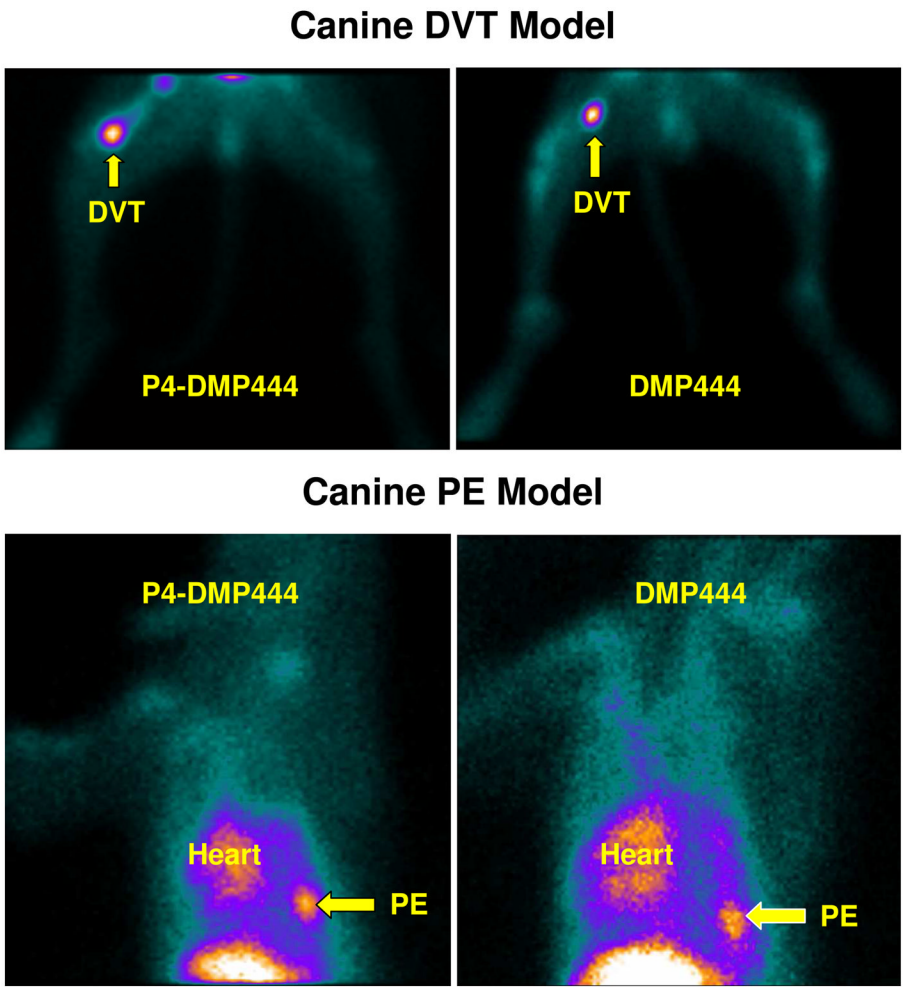

Figure 5.
Top: planar images of lower body parts of the dogs with DVT in their right thigh at 120 min after injection of DMP444 (right) and P4-DMP444 (left). Bottom: planar images of chest region of the dog with PE in the right lung at 120 min after injection of DMP444 (right) and P4-DMP444 (left). The blood pool radioactivity in the heart was higher for DMP444 than that for P4-DMP444.

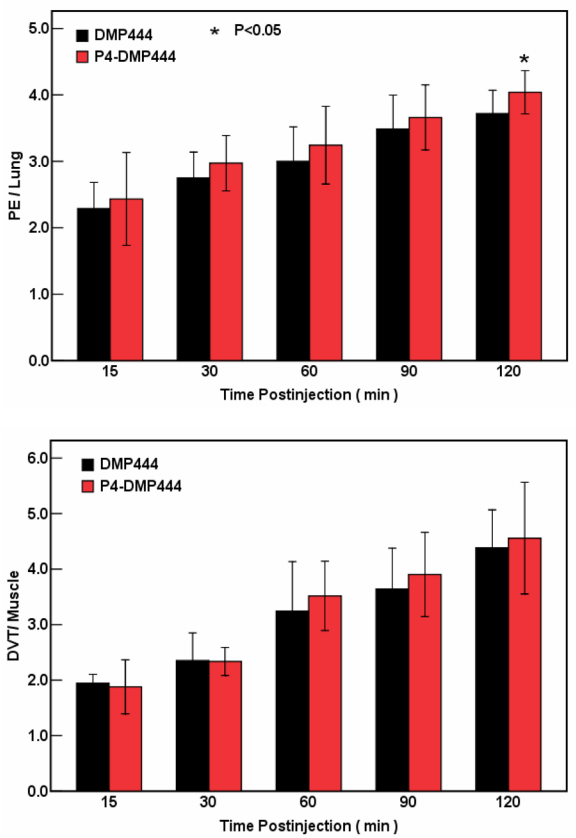

Figure 6.

Comparison of PE/lung and DVT/muscle ratios for DMP444 (n = 5) and P4-DMP444 (n = 5) in dogs. The PE/lung ratio of ^{99m}Tc-P4-DMP444 was significantly better than that of DMP444 at 120min p.i. There was no significant difference between DMP444 and P4-DMP444 for their DVT/muscle ratios.

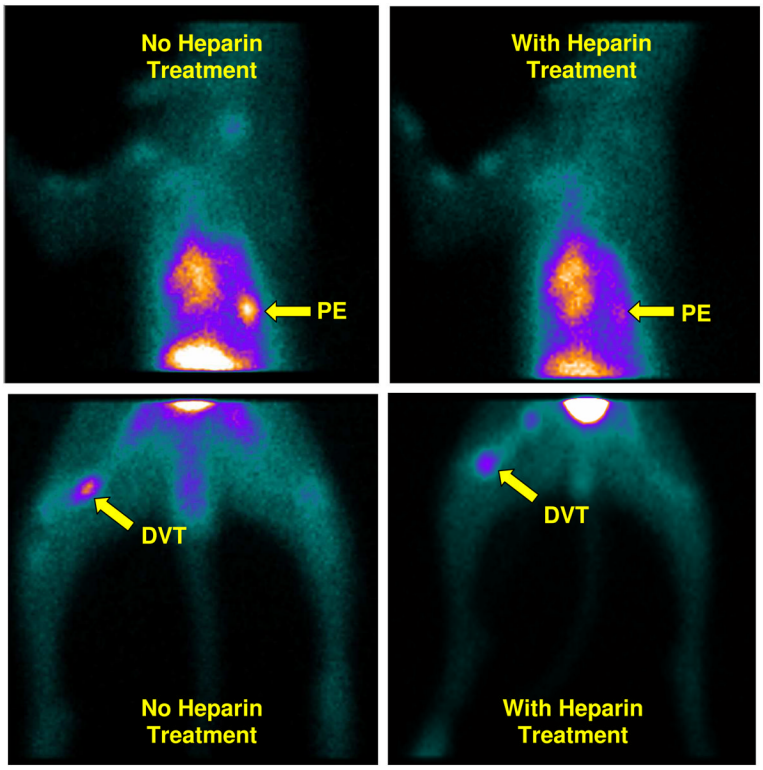

Figure 7.
Planar images of the dogs with PE in the right lung (top) and DVT in their right thighs (bottom) at 120 min after injection of P4-DMP444 with (right) and without (left) the anti-thrombosis treatment with heparin (200 units/kg). Arrows indicate the presence of thrombus.